The $\pi h_{11/2} \otimes \nu h_{11/2}$ yrast band in odd-odd ^{140}Tb

M. A. Rizzutto
Departamento de Ciências Exatas e Tecnológicas, Faculdades Integradas de Guarulhos, Guarulhos, SP, Brazil

M. N. Rao, W. A. Seale, J. R. B. Oliveira, E. W. Cybulska, N. H. Medina, and R. V. Ribas
Instituto de Física, Universidade de São Paulo, São Paulo, SP, Brazil

F. R. Espinoza-Quiñones
Centro de Engenharia e Ciências Exatas, Universidade Estadual do Oeste do Paraná UNIOESTE, Toledo, PR, Brazil

D. Bazzacco, F. Brandolini, S. Lunardi, C. M. Petrache, Zs. Podolyák, C. Rossi-Alvarez, and C. A. Ur
Dipartimento di Fisica dell'Università and INFN, Sezione di Padova, Padova, Italy

G. de Angelis, D. R. Napoli, P. Spolaore, A. Gadea, D. De Acuña, M. De Poli, E. Farnea, D. Foltescu,
M. Ionescu-Bujor,* and A. Iordachescu*
INFN, Laboratori Nazionali di Legnaro, Legnaro, Italy

A. Chatterjee and A. Saxena
Bhabha Atomic Research Center, Bombay, India

L. Sajo Bohus
Instituto de Fisica, Universidad Simon Bolivar, Caracas, Venezuela
(Received 13 April 2000; published 20 July 2000)

The $\pi h_{11/2} \otimes \nu h_{11/2}$ yrast band in the odd-odd nucleus ^{140}Tb has been populated by the ^{92}Mo (^{54}Fe, αpn) reaction at 240-MeV incident beam energy. No previous spectroscopic information was known in this nucleus. The present data fit nicely in the systematics of the $N=75$ isotones of La, Pr, Pm, Eu, and Tb ($Z=57$ to 65).

PACS number(s): 21.10.Re, 23.20.En, 23.20.Lv, 27.60.+j

In order to investigate neutron-deficient nuclei in the $A \approx 140$ mass region we have carried out a study of the ^{54}Fe $+ ^{92}$Mo reaction at 240-MeV incident beam energy. The incident beam was obtained with the XTU tandem accelerator of the Legnaro National Laboratory, Legnaro, Italy. The multidetector array GASP [1], consisting of 40 high-efficiency Compton-suppressed HpGe detectors and the 80-element BGO multiplicity filter, was used for obtaining gamma-ray double and triple coincidence spectra. The 40-telescope Si ball (ISIS) [2] permitted information on the type and multiplicity of the charged particles emitted, while the recoil mass spectrograph [3] allowed mass identification. The target used was an ≈ 1 mg/cm^2 thick ^{92}Mo foil.

Due to the fact that the efficiency of charged particle detection of the ISIS ancillary detector is not 100%, the observed charged particle (type and multiplicity) gated spectra contain transitions from different channels. For example, events from $\alpha 2p$ (^{140}Gd), $\alpha 3p$ (^{139}Eu), $2\alpha p$ (^{137}Eu), and the $2\alpha 2p$ (^{136}Sm) channels will appear in αp (^{141}Tb) spectra, due to the escape from detection in the charged particle array of one or more protons and alpha particles. The αpn events will also appear in the αp spectra, as there was no neutron detection. Thus, one can represent each multiplicity gated γ-γ matrix as a weighted superposition of several individual channels, each with a weight proportional to the intensities of gamma rays representing the particular channel. This leads to a set of linear equations which may be solved to obtain linear combinations of the various spectra which then consist of transitions belonging only to the given channel of interest. We have used this technique to generate ''cleaned'' spectra consisting of transitions from each individual reaction channel corresponding to the various charged particle multiplicities.

To illustrate the resulting ''cleaned'' spectra in the present case, we show in Fig. 1(a) the αp-gated γ-γ total projected spectrum, obtained from the charged-particle (type and multiplicity)-γ-γ cube. The gamma-ray peaks corresponding to ^{140}Gd ($\alpha 2p$), ^{139}Eu ($\alpha 3p$), ^{137}Eu ($2\alpha p$), and ^{136}Sm ($2\alpha 2p$) channels can also be seen in this spectrum, in addition to the transitions in ^{141}Tb and ^{140}Tb nuclei produced in the αp and αpn channels. The ($\alpha 2p$) channel is the strongest of these four channels, while the other three are populated much more weakly. In Fig. 1(b) the contributions of the peaks from channels other than αp and αpn have been clearly suppressed by the procedure described above. For example, in Fig. 1(b) the strongest lines corresponding to γ ray transitions from the yrast band of ^{140}Gd ($\alpha 2p$ channel) have disappeared, while those belonging to ^{141,140}Tb (αp and αpn channels) are enhanced.

Of the various nuclei ($Z=63$ to 66; $N=75$ to 78) produced in this experiment, the $3p$ channel leading to ^{143}Tb

*Permanent address: Institute of Physics and Nuclear Engineering, Bucharest, Romania.

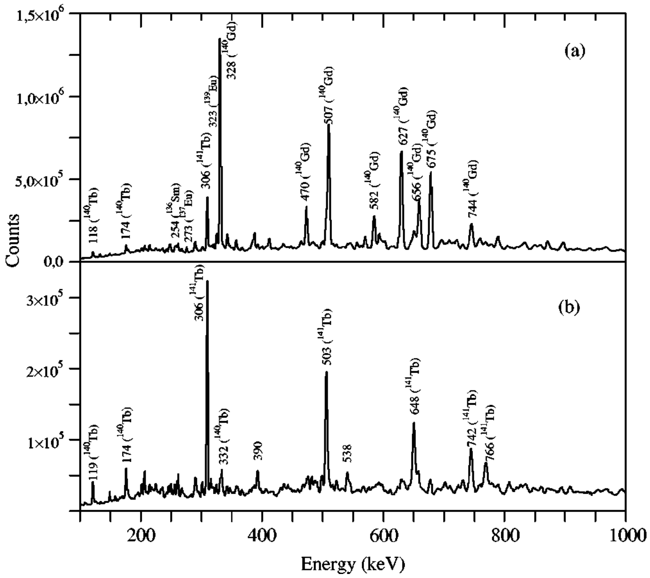

FIG. 1. (a) αp-gated γ-γ total projected spectrum. (b) ''Cleaned'' αp and αpn spectra from which the contributions of $x\alpha yp$ $(x,y \geqslant 2)$ channels have been removed.

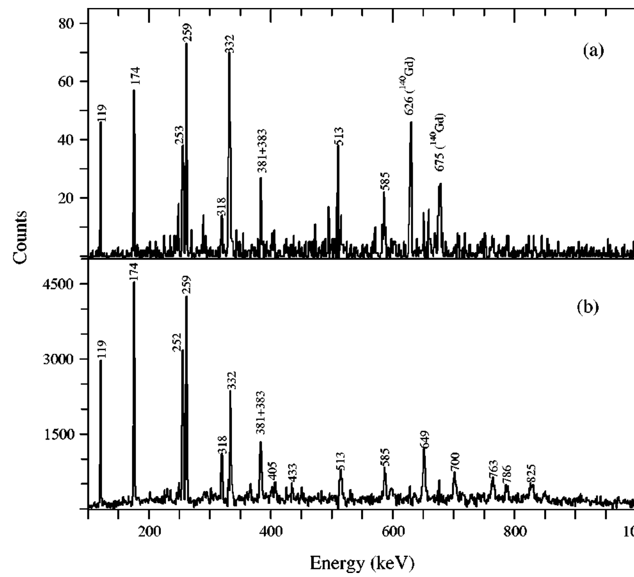

FIG. 2. (a) Sum of gates on several transitions assigned to ^{140}Tb starting with $(A=140)$-γ-γ cube. (b) Sum of gates on several transitions assigned to ^{140}Tb starting with the ''cleaned'' charged-particle (type and multiplicity)-γ-γ cube.

was the strongest one populated at the incident energy used and the results on the high-spin structures populated in ^{143}Tb were described in [4], where a more detailed description of the experiment and the analysis of data may be found. We report here the results on the αpn channel leading to the odd-odd nucleus ^{140}Tb. No data on high-spin states were known in ^{140}Tb previous to this work. In spite of the fact that the production cross section for this nucleus was about one tenth that of ^{143}Tb and about a third of the αp channel leading to ^{141}Tb, it was possible to unambiguously assign gamma transitions to ^{140}Tb nucleus by ruling out the possibility of these transitions belonging to ^{141}Tb, based on the mass-gated spectra. In Fig. 2(a) we present the spectrum of gamma rays, obtained as a sum of gates on several gamma transitions assigned to ^{140}Tb from an analysis of the mass-gated matrices. The spectrum in Fig. 2(b) was generated in a similar manner, except for the fact that we started with the ''cleaned'' charged-particle (type and multiplicity)-γ-γ cube, instead of the A-γ-γ cube, in order to obtain better statistics.

The level scheme of ^{140}Tb obtained from the present work is shown in Fig. 3, while Fig. 4 presents the $[\pi h_{11/2} \otimes \nu h_{11/2}]$ band in ^{140}Tb $(Z=65)$ compared with the corresponding bands in the odd-odd nuclei with $Z=57-63$, ^{132}La [5], ^{134}Pr [6–8], ^{136}Pm [6], and ^{138}Eu [9]. One can see the smooth behavior of the excitation energies among the 5 isotones above the level with a spin and parity assignment of (8^+). This smooth trend would continue down one more level, fed by the 118-keV γ ray in ^{140}Tb which could then be the assigned (7^+) spin and parity, based on the DCO ratio of the 118-keV transition [1.13 (20), see Table I]. This assignment would then be consistent with the smooth systematics of all the previous level schemes and spin assignments for the $[\pi h_{11/2} \otimes \nu h_{11/2}]$ bands in the $N=75$ doubly odd isotones. The only exception to this behavior would then be the level scheme of ^{134}Pr according to [8], where there is a cascade of two gamma rays viz., 306.5- and 94.3-keV deexciting the (8^+) level, instead of just a single γ ray of $M1$ multipolarity. No $(9^+ \rightarrow 7^+)$ transition has been observed in the $[\pi h_{11/2} \otimes \nu h_{11/2}]$ bands in any of these nuclei, except in the case of ^{134}Pr [8], where it was observed as a very weak 477.2-keV transition $(<0.5\%)$ and with only a tentative placement in the level scheme. In addition there is disagreement in the placement of the 306.5-keV gamma ray between [6] and [8]. We also mention here that recently Liu *et al.* [10] have published a systematic study of spin assignments of low-lying levels in doubly odd nuclei around $A \approx 130$. The

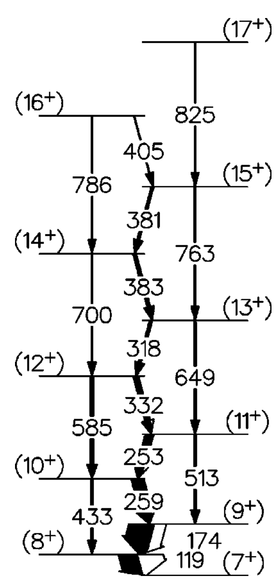

FIG. 3. The level scheme of ^{140}Tb obtained from the present work.

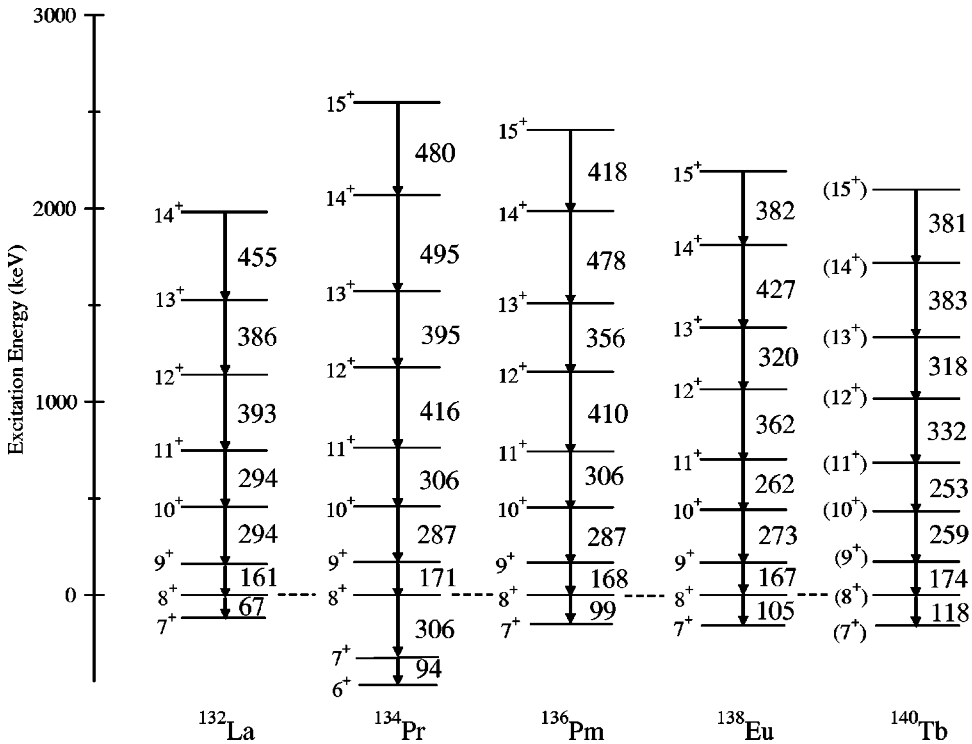

FIG. 4. The $[\pi h_{11/2} \otimes \nu h_{11/2}]$ bands in the odd-odd $N=75$ isotonic chain with $Z=57$–65.

authors base their conclusions on the argument that the excitation energy of the levels in the $[\pi h_{11/2} \otimes \nu h_{11/2}]$ bands, with the same assigned spin, in a chain of deformed doubly odd isotones (isotopes) varies with the proton (neutron) number in a smooth way, and a deviation from this smooth trend may imply a questionable spin assignment. They then go on to consider that the correct spin assignment is that which removes the deviation from the smooth trend. In the mass region of $A \approx 130$, these authors suggest that the spins of the levels of the $[\pi h_{11/2} \otimes \nu h_{11/2}]$ bands may differ by one unit from those shown in Fig. 4. Such a possibility cannot be confirmed or overruled from the present data.

The energy levels, transition energies, intensities and DCO ratios and tentative spin and parity assignments for the levels assigned to the ^{140}Tb nucleus are shown in Table I. The DCO ratios shown have been obtained with gates on dipole transitions, and as such, one would expect a value of 1.0 for a dipole and 2.0 for a quadrupole transition for the

TABLE I. Energy levels, transition energies, intensities, DCO ratios, and tentative spin and parity assignments for the levels assigned to the ^{140}Tb nucleus.

E_γ [keV]	E_i [keV]	E_f [keV]	$I_i^\pi \rightarrow I_f^\pi$	I_γ	DCO ratio
118.7	118.7	0	$(8^+) \rightarrow (7^+)$	100	1.13 (20)
173.7	292.4	118.7	$(9^+) \rightarrow (8^+)$	94	1.0 (1)
253.5	805.4	551.9	$(11^+) \rightarrow (10^+)$	27	0.94 (13)
259.5	551.9	292.4	$(10^+) \rightarrow (9^+)$	41	0.75 (8)
317.6	1454.7	1137.2	$(13^+) \rightarrow (12^+)$	10	1.03 (18)
331.8	1137.2	805.4	$(12^+) \rightarrow (11^+)$	19	0.68 (17)
380.8	2217.9	1837.1	$(15^+) \rightarrow (14^+)$	9	
382.6	1837.1	1454.7	$(14^+) \rightarrow (13^+)$	12	
405.0	2622.9	2217.9	$(16^+) \rightarrow (15^+)$	< 5	
433.2	551.9	118.7	$(10^+) \rightarrow (8^+)$	6	
513.0	805.4	292.4	$(11^+) \rightarrow (9^+)$	7	
585.3	1137.2	551.9	$(12^+) \rightarrow (10^+)$	12	1.89 (44)
649.3	1454.7	805.4	$(13^+) \rightarrow (11^+)$	5.5	
699.8	1837.1	1137.2	$(14^+) \rightarrow (12^+)$	5.1	
763.2	2217.9	1454.7	$(15^+) \rightarrow (13^+)$	5.9	
785.9	2622.9	1837.1	$(16^+) \rightarrow (14^+)$	< 5	
825.0	3042.9	2217.9	$(17^+) \rightarrow (15^+)$	< 4	

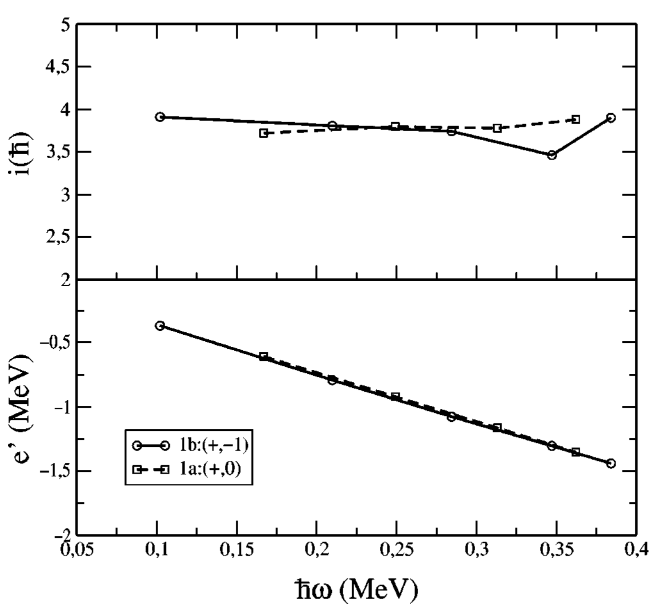

FIG. 5. The experimental alignments i_x and Routhians e' for the two signature components, viz. $\alpha = -1$ and 0 of the yrast band of ^{140}Tb.

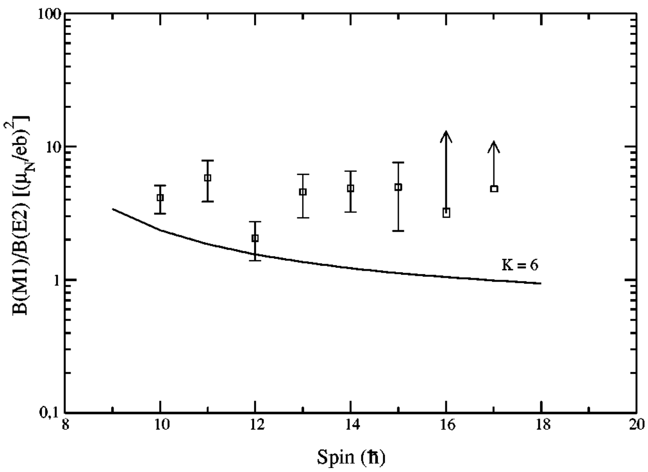

FIG. 6. The ratios of the reduced transition rates $B(M1)/B(E2)$ for the levels in the yrast band of ^{140}Tb.

GASP geometry [4]. The experimental alignments i_x and Routhians e' for the two signature components, viz., $\alpha = -1$ and 0 of the yrast band of ^{140}Tb were extracted by using a frequency-dependent reference $\mathcal{J}_{\mathrm{ref}} = 20.0 + 67.0\omega^2$ ($\hbar^2$ MeV^{-1}), extracted from the data. These results have been presented in Fig. 5. The signature splitting is less than about 25 keV for rotational frequencies below $\hbar\omega = 0.3$ MeV, similar to that observed in the other isotones. This has been attributed to a small amount of triaxiality ($\gamma \approx -10°$ to $-15°$) in nuclei of this mass region.

From the intensities of $M1$ and $E2$ transitions in the band, the ratios of the reduced transition rates $B(M1)/B(E2)$ have been obtained, assuming that the $E2/M1$ mixing ratio δ for the $\Delta I = 1$ transitions is zero. It is found (Fig. 6) that the ratios of the reduced transition rates are about $4.0 \pm 1.5(\mu_N/e\,\mathrm{b})^2$. Similar values have been found for the other nuclei in the isotonic chain [6,9]. Also shown in Fig. 6 is the theoretical estimate of these ratios, obtained using the geometrical model [11], for the $\pi h_{11/2} \otimes \nu h_{11/2}$ configuration for $K = 6$ (corresponding to $\omega_n = 9/2$; $\omega_p = 3/2$). A value of $K = 7$ ($\omega_p = 5/2$) leads to very similar results.

In summary, the yrast band has been located in the doubly-odd ^{140}Tb for the first time. Its structure is very similar to corresponding bands in lighter doubly-odd isotones with two high-j quasiparticles, pointing to the stabilizing effect of these quasiparticles on the γ-soft cores.

We thank G. Manente for the preparation of the targets, and the staff of the XTU-Tandem of LNL for the smooth operation of the accelerator. This work was partially supported by the Fundação de Amparo à Pesquisa do Estado de São Paulo (FAPESP) and the Conselho Nacional de Desenvolvimento Científico e Tecnológico (CNPq), Brazil.

[1] D. Bazzacco, in Proceedings of the International Conference on Nuclear Structure at High Angular Momentum, Ottawa, 1992, Report No. AECL 10613, Vol. 2, p. 376.
[2] E. Farnea *et al.*, Nucl. Instrum. Methods Phys. Res. A **400**, 87 (1998).
[3] P. Spolaore, J. D. Larson, C. Signorini, S. Beghini, Z. Xi-Kai, and S. Hou-Zhi, Nucl. Instrum. Methods Phys. Res. A **238**, 381 (1985).
[4] F. R. Espinoza-Quiñones *et al.* Phys. Rev. C **60**, 054304 (1999).
[5] J. R. B. Oliveira, L. G. R. Emediato, M. A. Rizzutto, R. V. Ribas, W. A. Seale, M. N. Rao, N. H. Medina, S. Botelho, and E. W. Cybulska, Phys. Rev. C **39**, 2250 (1989).
[6] C. W. Beausang, L. Hildingsson, E. S. Paul, W. F. Piel, Jr., P. K. Weng, N. Xu, and D. B. Fossan, Phys. Rev. C **36**, 1810 (1987).
[7] C. M. Petrache, G. de Angelis, D. Bucurescu, M. Ivascu, D. Bazzacco, and S. Lunardi, Z. Phys. A **344**, 227 (1992).
[8] C. M. Petrache, D. Bazzacco, S. Lunardi, C. Rossi Alvarez, G. de Angelis, M. De Poli, D. Bucurescu, C. A. Ur, P. B. Semmes, and R. Wyss, Nucl. Phys. **A597**, 106 (1996).
[9] Y. Liang, K. Ahn, R. Ma, E. S. Paul, N. Xu, and D. B. Fossan, Phys. Rev. C **38**, 2432 (1988).
[10] Y. Liu, J. Lu, Y. Ma, S. Zhou, and H. Zheng, Phys. Rev. C **54**, 719 (1996).
[11] F. Dönau and S. Frauendorf, in *Proceedings of the Conference on High Angular Momentum Properties of Nuclei*, Oak Ridge, 1982, edited by N. R. Johnson (Harwood Academic, New York, 1983), p. 143; F. Dönau, Nucl. Phys. **A471**, 469 (1987).